Calibration of speleothem $\delta^{18}O$ with instrumental climate records from Turkey

Catherine N. Jex [a,b,*], Andy Baker [a], Ian J. Fairchild [a], Warren J. Eastwood [a], Melanie J. Leng [b,c], Hilary J. Sloane [b], Louise Thomas [d], Erdem Bekaroğlu [e]

[a] School of Geography, Earth and Environmental Sciences, The University of Birmingham, Birmingham B15 2TT, UK
[b] NERC Isotope Geosciences Laboratory, British Geological Survey, Keyworth, Nottingham, NG12 5GG, UK
[c] School of Geography, University of Nottingham, Nottingham, NG7 2RD, UK
[d] Faculty of Science, Open University, Walton Hall, Milton Keynes, MK7 6AA, UK
[e] Department of Geography, Ankara University, 06100, Sihhiye, Ankara, Turkey

ARTICLE INFO

Article history:
Received 27 October 2008
Accepted 20 August 2009
Available online 6 September 2009

Keywords:
speleothem
climate calibration
stable isotopes
Turkey

ABSTRACT

Stalagmite records of oxygen ($\delta^{18}O$) isotopes, sampled at sub-annual resolution by micro-mill techniques are correlated with climate parameters over the instrumental period (1961 to 2005 AD). The strongest correlations were found between $\delta^{18}O$ and total amount of late autumn–winter precipitation (October to January) smoothed by 6 yr, with marginally weaker correlations between the total amount of late autumn–spring precipitation (ONDJF and ONDJFMA) smoothed over the same time period. Two smoothing options were chosen to account for variability in mixing and residence times of stored water in the karst aquifer prior to entering the cave: (1) An average of the last 6 yr of precipitation which yielded a product correlation of −0.71 for the months ONDJ; and (2) a mixing model of 10% short term/event water (<1 yr) and 90% water of a longer residence time in the karst aquifer (2 to 6 yr) which gave a product correlation of −0.72 for the months ONDJ. Precipitation is calibrated over the instrumental period (1961 to 2004 AD) based on linear regression of $\delta^{18}O$ with observed precipitation for the months ONDJ, ONDJF and ONDJFMA using both smoothing methods. An uncertainty of ±31 mm (2 standard errors on the linear regression) is applied to the calibrations. This is the first speleothem calibration of its kind in Turkey.

1. Introduction

The focus of palaeoclimate research over the last two decades has been to obtain proxy records of climatic parameters (temperature and precipitation) beyond the maximum length of direct measurements available from instrumental records. This is necessary to put recent trends observed in the instrumental records, specifically reductions in water availability and increased aridity in the mid-latitudes and in semi-arid low latitude regions (IPCC, 2007), into a longer temporal context. Speleothems in particular, offer a good possibility of defining continuous high resolution records of past precipitation by way of calibration of annually resolved proxy data with local instrumental records.

Published speleothem records are rare in Turkey and to the authors' knowledge only two paleoenvironemntal publications using Turkish speleothems currently exist. Frisia et al (2008) report the response of stalagmite $\delta^{13}C$ and S content to the Santorini eruption ca. 3350–3800 BP, using a stalagmite from NW Turkey; and Krüger et al. (2008) demonstrate the application of temperature reconstruction from fluid inclusions from the modern period of deposition of the same stalagmite. Speleothems are deposited in caves by the degassing of drip waters saturated for $CaCO_3$ after percolating down through the karst aquifer (Ford and Williams, 2007). They are increasingly popular sources of proxy records for palaeoclimate reconstructions, since the factors controlling their growth rate and the nature of their internal structure and chemical composition respond to changes in surface climate (Baker et al., 1998; McDermott, 2004; Fairchild et al., 2006; Banner et al., 2007). The main controls on the growth rate of a speleothem are supersaturation of cave water driven by degassing due to a pCO_2 gradient between drip waters and cave air. Controls on these processes include: ventilation, cave temperature and rate of water discharge (Dreybrodt, 1988). As such, speleothems are capable of recording a modified climate signal, smoothed by the mixing of waters of different ages within the karst aquifer before entering the cave as drip water (McDermott, 2004; McDermott et al., 2006; Fairchild et al., 2006), via a number of measurable proxies. Stable isotope ratios ($\delta^{18}O$ and $\delta^{13}C$) are commonly used to obtain palaeoenvironmental information from speleothems and thorough reviews of their application in speleothem research are available. Specifically, McDermott (2004) and Fairchild et al. (2006) are amongst the most recent. The oxygen isotope ($\delta^{18}O$) composition of precipitation falling on the surface above the cave is a function of several "effects", including air temperature, amount of rainfall, amount of rainout prior to reaching the cave site, and on glacial time scales, global ice volume effect.

* Corresponding author. School of Geography, Earth and Environmental Sciences, The University of Birmingham, Birmingham B15 2TT, UK. Tel.: +44 (0) 121 414 5523.
E-mail addresses: c.jex@bham.ac.uk (C.N. Jex), a.baker.2@bham.ac.uk (A. Baker), mjl@bgs.ac.uk (M.J. Leng), hjs@bgs.ac.uk (H.J. Sloane), L.E.Thomas@open.ac.uk (L. Thomas), bekaroglu@humanity.ankara.edu.tr (E. Bekaroğlu).

0921-8181/$ – see front matter © 2009 Elsevier B.V. All rights reserved.
doi:10.1016/j.gloplacha.2009.08.004

As this rainfall penetrates into the soil and into the karst aquifer, its isotopic value may be modified by way of evaporation at the surface or in air pockets in the karst aquifer. In the lower epikarst, the rate of infiltration and mixing of older stored waters and younger "event" waters may further dampen the high-frequency signal (Fairchild et al., 2006). Finally, high-frequency noise may be introduced into the isotopic signal due to a number of kinetic effects during calcite precipitation and is often identifiable by some simple tests for co-variation of $\delta^{18}O$ and $\delta^{13}C$ and progressive enrichment along individually precipitated lamina within the stalagmite (Hendy, 1971). An understanding of how the stable isotope signal of infiltrating drip waters is modified en-route from surface to cave is essential in palaeoenvironmental investigations of $\delta^{18}O$ (and $\delta^{13}C$) in speleothems and is traditionally obtained by modern monitoring of the cave environment. This may involve collection of surface waters and cave waters of various hydrological settings, for trace element and isotope analysis, and cave microclimate measurements (Treble et al., 2005; Fuller et al., 2008). More recently, Baker et al. (2007) obtained a quantitative reconstruction of palaeo-rainfall in Ethiopia since 1910 by correlating annually sampled stable isotope data with contemporaneous instrumental records of rainfall, using simple linear regression and methods of smoothing the data to account for mixing times in the karst aquifer. A review of such methods is provided by Baker and Bradley (2010-this issue). To date, only a limited number of quantitative speleothem proxy-climate calibrations exist due to the need for a robust chronological control, namely the presence of annual lamination. A recent review by Lachniet (2009) describes only three successful attempts to calibrate speleothem $\delta^{18}O$ with climate parameters.

This study presents the results from a stalagmite removed from Akçakale cave in the Gümüşhane province of NE Turkey. We obtained an annually resolved speleothem and calibrated stable isotope data with contemporaneous local instrumental records. We show that the stable isotope composition of speleothem calcite, in this case, is most responsive to late autumn–winter (ONDJ) precipitation.

2. Regional setting of Akçakale cave

Akçakale cave is located on the landward side of the tectonically-active Black Sea Mountains in the Gümüşhane province of north-east Turkey (Fig. 1). It is located at an altitude of 1530 m asl and developed in Jurassic–lower Cretaceous limestone (Nazik, 1994). Regional uplift during the Barremian stage (125 to 130 Ma) resulted in widespread karstification creating the many caves that exist today (Robinson et al., 1995).

Akçakale cave (Fig. 1) has a narrow, man-made, entrance level, which declines into a vast central chamber. The chamber contains many large "pancake-like" stalagmite formations, produced as a result of the large distance from cave ceiling to floor. The entrance was made by exploding the exterior of the mountain, and as a result many large speleothems, have collapsed and now cover the cave floor. It is a hydrologically active cave with fast flowing water features and drips. A lake has formed in the northern end of the cave and there is a waterfall in the NNW end of the central chamber. There are many flowstones and curtains/pillar formations within the cave and there are areas of clay which are likely the result of flooding during winter and spring. Akçakale drip rates range from 3 to 70 s drip^{-1} with some drips observed as continuous or almost continuous flows with drip rates greater than 1 s drip^{-1}. Recharge to the karst aquifer above Akçakale is thought to be predominantly sourced from precipitation falling between autumn to spring, with a large input from spring melt of winter precipitation (Section 4.2). Relative humidity (RH) in the area of

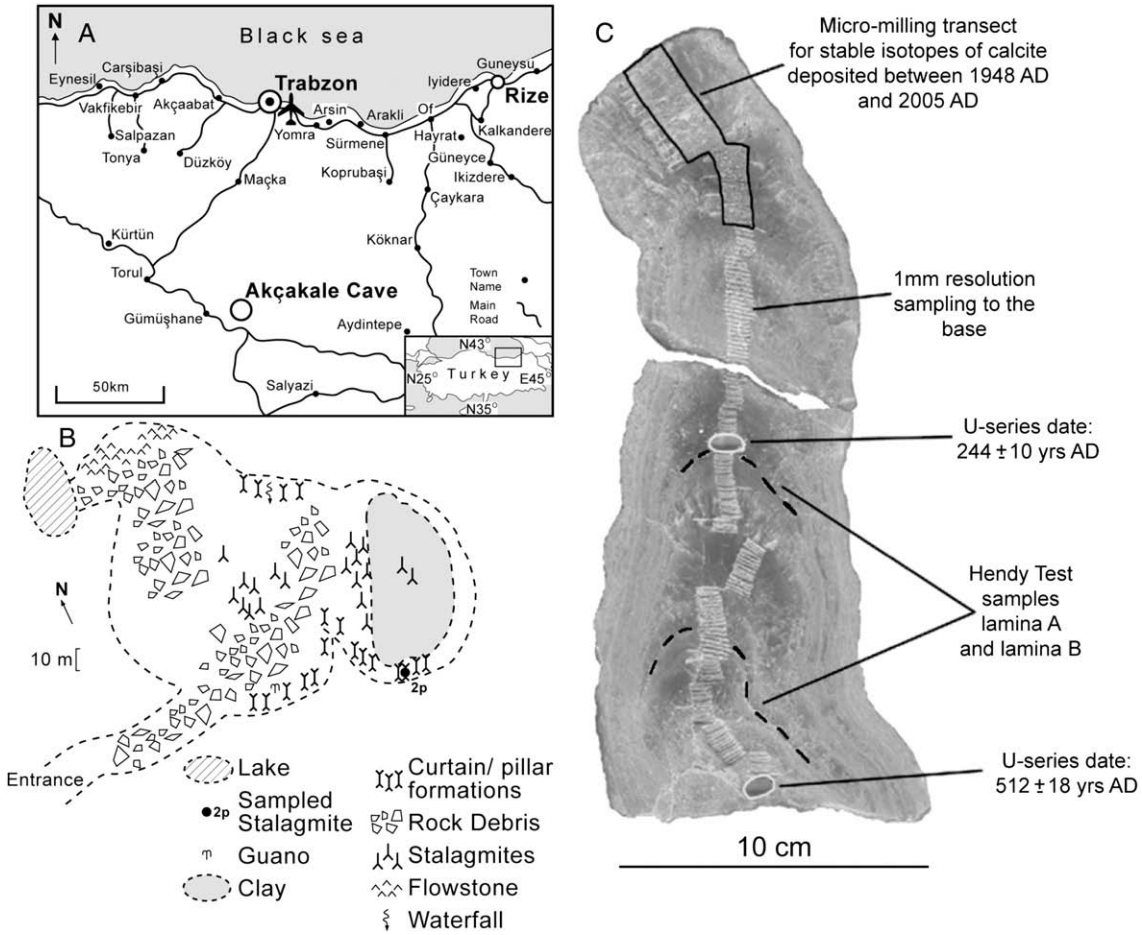

Fig. 1. A: Location of Akçakale cave in Gümüşhane province, NE Turkey; cave altitude 1530 m asl. B: Schematic plan of Akçakale cave. C: Cross-sectioned surface of stalagmite 2p showing internal laminae and sampling locations.

the cave where stalagmites were removed was around 98% at the time of removal. RH at around this level reduces the likelihood of fractionation between drip waters and stalagmite calcite due to evaporation (Mickler et al., 2004). Cave air CO_2 concentrations of 800 to 950 ppm were recorded during a two week monitoring period in July 2005.

The land surface directly above the area in the cave from where the stalagmites were removed has a soil depth of ~30 cm, though parts are stable vegetated scree. Tree growth exists in what appears to be a dried up river bed and there is evidence of farming in close proximity (ploughed field). Around the cave entrance there is exposed limestone bedrock.

3. Materials and methods

A lamina chronology of stalagmite 2p (Figs. 1 and 2) was established by counting visible laminae on the polished halves of the stalagmites, imaged by conventional microscopy under visible light. Images of a transect following the central growth axis of the stalagmite were taken using a low power Zeiss stemi SV 11 microscope (at 0.6–6.6× magnification), a Schott 1500 LCD light source (15 V/150 W) and a "Q-imaging" MicroPublisher 5.0 RTV camera. The laminae were counted and their thickness from the base of one DCC lamina to the top of a WPC lamina was measured as one lamina (Genty et al., 1997) using Image Pro Plus, version 6 software. Where possible, multiple growth rates were measured across a lamina and averaged to give a mean thickness.

For dating by U-series (location in Fig. 1), 0.5 g (±~0.05 g) of calcite powder were drilled from a fresh clean surface (cleaned with 2% HCl, then rinsed with de-ionized water) using a hand held dentist's mini drill (COMO Drills, microturbo 1) with diamond tipped drill bits (0.5 mm diameter as supplied with drill). Drilled samples were prepared by wet column chemistry to separate Th and U fractions prior to loading onto graphite coated Re filaments, and analysed on a Finnigan MAT262-II Thermal Ionization Mass Spectrometer. ^{238}U-concentrations of 0.54 to 0.58 ppm are observed in 2p. Low ^{230}Th/^{232}Th activity ratios (up to 23.5) suggest non-negligible detrital Th. In the first instance a detrital correction ratio (^{232}Th/^{238}U) of 3.12 (i.e. bulk earth) was applied, which results in the corrected date given in Table 1 and shown in Fig. 2. Varying the initial detrital ^{232}Th/^{238}U between 0.3 and 18, a range reported to occur in speleothems (Smith, 2006) results in a larger error of +28/−53 yr, defining the most conservative error estimates on this date.

Stalagmite 2p (Fig. 1) was fed by an actively dripping stalactite when removed from Akçakale cave in July 2005, and since its removal calcite has been precipitated on a tile that was put in its place in order to confirm active calcite precipitation. Stalagmite (2p) is 198 mm in length along its central growth axis and comprises porous calcite throughout, with regions of more compact darker brown calcite. From the top of 2p there are 107 continuous visible laminations, observed to a depth of 56.7 mm (Fig. 2) and comparable in nature to white porous calcite/dark compact calcite (WPC/DCC) laminae as described by Genty et al. (1997). Mean lamina thickness is 0.52 mm lam^{-1} ($1\sigma = 0.33$) and falls in range of predicted growth rates of 0.69 mm lam^{-1} ($1\sigma = 0.35$) assuming a cave air temperature of 10 °C and Ca^{2+} concentration of 62 ppm in drip waters (Dreybrodt, 1988). Prior to this, 2p is discontinuously laminated and the chronology is constrained by the U–Th date at ~90 mm depth (Fig. 2). The orientation of the central growth axis changes throughout the depositional history of 2p, as it was removed from a curtain/drapery setting, and so a frequent change in routing of drip water to the feeding stalactite is likely. Drip rates averaged at 3.7 s drip^{-1} at the time of sampling and synthetic (predicted) SI_c (saturation index) is between 0 and +1. The strongly seasonal climate of the region (see Section 4.1) suggests the potential for annually laminated stalagmites (Tan et al., 2006; Baker et al., 2008). The annual nature of these visible laminae is supported by the agreement between measured and predicted growth rates, active calcite precipitation at the time of removal and the U–Th date at ~90 mm depth which itself confirms calcite precipitation since ~244 yr BP (BP = 2005 AD). Linear interpolation between lamina 107 to this date predicts growth rates ~0.4 mm yr^{-1}; again in range of those predicted and measured directly for this earliest part of 2p (Fig. 2).

High resolution sampling for stable isotopes was carried out using the micro-mill facilities at the Department of Earth Sciences, Oxford University. This was achieved by trench sampling along individual lamina according to the protocols of Fairchild et al. (2006). Drilling resolution was set at 0.1 and 0.4 mm to cover the instrumental time period (the last ~40 yr) for high resolution climate calibration. Milled calcite powder samples were weighed (60 μg) and analysed for stable isotopes δ^{13}C and δ^{18}O using an automated common acid bath VG Optima + ISOCARB mass spectrometer. Results are reported to VPDB and precision is ±0.1‰. Samples were drilled for Hendy tests using a hand held dentist drill (as described above), by the same trench sampling protocol along an individual lamina. Analysis for δ^2H and δ^{18}O of water samples (cave waters, surface waters and precipitation) was carried out using a GV Instruments Isoprime continuous-flow mass spectrometer and Eurovector EA (Elemental Analyzer) preparation line. Data are reported to VSMOW and precision is ±0.15‰ (δ^{18}O) and ±2‰ (δ^2H). Monthly records of mean temperature and precipitation totals at Gümüşhane meteorological station (WMO station code: 17088) were obtained from the Turkish State Meteorological Service. The records are largely continuous back to 1961, though no metadata were available to the authors at the time of publication.

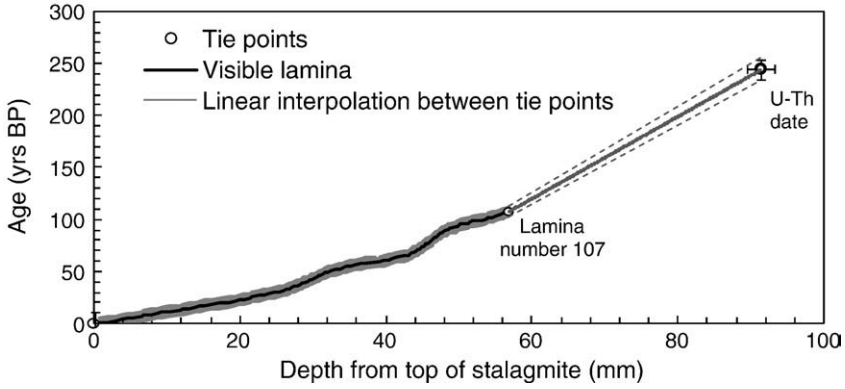

Fig. 2. Age–depth model for sample 2p. There are 107 countable lamina (solid black line) from 0 to ~60 mm depth from the top of the stalagmite. These provide two tie-points for the age–depth model. Each lamina over this section is assumed to represent 1 yr of calcite growth (see text). The third tie-point is the U–Th date at ~90 mm depth. Linear interpolation (grey solid line) between this tie-point and the last countable lamina at ~60 mm depth provides an age for this portion of the speleothem. Grey dotted lines represent the maximum and minimum age estimates of the linear interpolation (±10 yr). Grey shading represents a 4% error applied to lamina counts.

Table 1
U–Th dates for stalagmite 2p (uncertainties associated with each measurement/ratio and the error associated with each age are shown in brackets). The corrected ages shown here are those associated with a detrital correction ratio ($^{232}Th/^{238}U$) of 3.12.

Lab code	Depth (mm)	^{238}U ppm	$[^{234}U/^{238}U]$	^{234}U ppm	^{230}Th ppb	$\frac{^{232}Th}{ppb}$	$[^{230}Th/^{234}U]_{uncorr}$	$[^{234}U/^{238}U]_{uncorr}$	$[^{230}Th/^{232}Th]$	$\frac{Age_{uncorr}}{(yr\ BP)}$	$[^{230}Th/^{234}U]_{corr}$	$[^{234}U/^{238}U]_{corr}$	$\frac{Age_{corr}}{(yr\ BP)}$
2 pm	92	0.5758	2.6224	8.15E−05	0.000061	0.906	0.0024	2.622	23.492	268	0.00225	2.62321	244
(uncertainty)	(2.5)	(0.0009)	(0.0080)	(2.31E−07)	(0.000001)	(0.164)	(0.000034)	(0.0080)	(1.097)	(8)	(0.00004)	(0.01129)	10

4. Results

4.1. Modern climate at Akçakale cave

Akçakale cave is located in between the climate regions of the Black Sea (Mean annual temperature (MAT): +14 °C; T_{max}: +25 °C; T_{min}: +6 °C and total annual precipitation (TAP): 1200 mm yr^{-1}) and Eastern Anatolia (MAT: +7 °C T_{max}: +19 °C; T_{min}: −7 °C and TAP: 420 mm yr^{-1}) as defined by Unal et al. (2003). Mean monthly temperature, total precipitation and water excess, calculated using the formula of Thornthwaite (1948 and 1957) are illustrated in Fig. 3. The Black Sea region has a temperate climate, strongly affected by maritime influences throughout the year with the Black Sea Mountains providing orographic uplift along NW facing slopes to onshore sea-breezes, making this region the wettest in Turkey (annual precipitation totals of 1200 mm yr^{-1} with Trabzon meteorological station recording precipitation on 142 days of the year; Statistical yearbook of Turkey, 2002). The eastern Anatolian region has reduced precipitation, being on the southern side of the Black Sea Mountains and reduced minimum temperatures as it is generally at higher altitudes (>1000 m asl).

Circulation may be characterised as westerly to north-westerly in winter (Kutiel et al., 1998) due to the presence of a seasonal Asian high and a high pressure ridge from the Azores to the west (Kadıoğlu, 2000). Depressions formed over the Mediterranean and Balkans affect the Mediterranean and Black Sea coasts as they move inland and result in heavy precipitation after orographic uplift by the Taurus and then the Black Sea mountain ranges. In spring circulation is north-westerly and occasionally weak easterly as the Asian high weakens (Kutiel et al., 1998). During the summer the Asian low draws down winds from the north/north-west, known as Meltum winds and in the autumn, northerly circulation brings warm moist air to the Black Sea region (Kutiel and Maheras, 1998; Kutiel et al., 2001).

Mean monthly temperature data at Gümüşhane (the nearest meteorological station to Akçakale) are shown in Fig. 3A, and range from −2 °C in January to +22 °C July and August (since 1961 AD). Calculated water excess for Gümüşhane (using the Thornthwaite formula: see figure captions for details) is shown in Fig. 3B and suggests a soil moisture deficit during June, July, August and September. Recharge to the karstic aquifer is most likely to occur during late autumn, winter and in early spring. However, as winter temperatures are often at or below zero degrees centigrade it is likely that snow melt and spring precipitation may comprise the main source of recharge waters to the karst aquifer.

4.2. Stable isotopes of modern precipitation and Akçakale cave waters

The Global Network of Isotopes in Precipitation (GNIP) data (IAEA/WMO, 2006) for nearby stations at Dalbahace, Senyurt and Sinop, along with the isotope values of surface waters and cave waters are shown in Fig. 3C. The GNIP data for these stations is discontinuous and sparse, collected between 1990 and 1993 AD. The single summer rain sample (−5.6‰) obtained during this study (2005 AD) plots away from the cave (−13.6 to −14.4‰) and surface waters (−12.7 to −15.3‰), and falls within the range of values recorded at GNIP stations during summer months of June, July and August when precipitation typically has $\delta^{18}O$ values greater than −7‰. All other collected samples plot slightly above the local meteoric water line for Turkey (LMWL(T)). Cave (and spring, stream and river) waters lie within ranges typical of winter snow and spring/autumn rain for this region, and are similar to the values of the snow-pack (−14.4‰) which represents typical winter accumulation. Further, the cave waters are typical of air masses of eastern Mediterranean origin and maritime polar/arctic air masses originating in central Europe (travelling over the Black Sea to this region, Dirican et al., 2005).

Using known values of cave temperature and the measured $\delta^{18}O$ of modern calcite ($\delta^{18}O_c$) (i.e. the top 1 mm) of stalagmite 2p, the

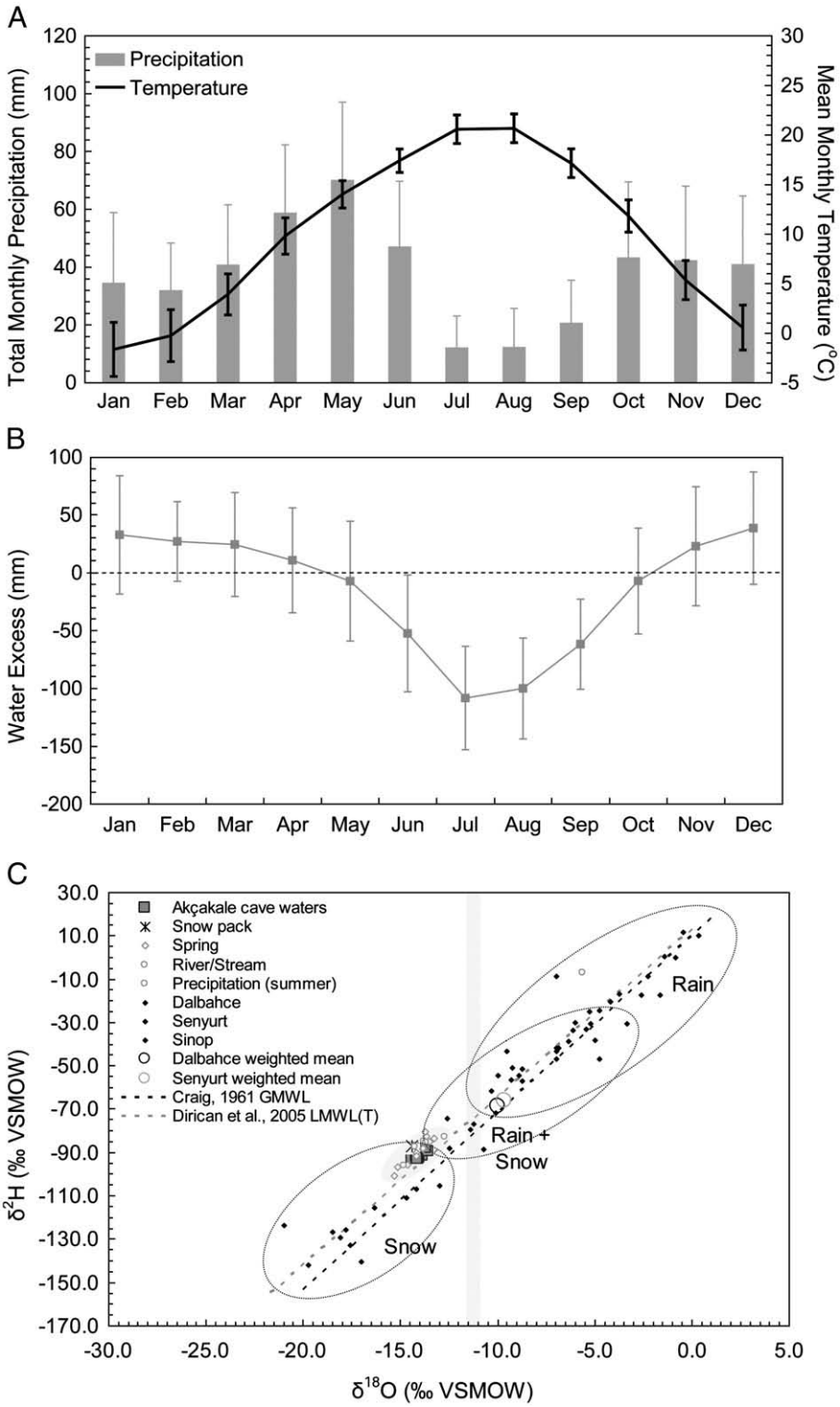

Fig. 3. A: Mean monthly temperature (AD 1961 to 2006) and total monthly precipitation (AD 1965 to 2006) recorded at Gümüşhane meteorological station; B: Monthly water excess (WE) calculated according to Thornthwaite (1948 and 1957) and applied using the assumptions of Genty and Deflandre (1998). C: Stable isotope water chemistry of precipitation obtained from the GNIP data-base for nearby stations: Dalbahace (39.31°N, 41.49°E, 1695 m asl; ~200 km east of Akçakale cave), Senyurt (39.38°N, 41.01°E, 2160 m asl; ~200 km east of Akçakale cave) and Sinop (42.03°N, 35.17°E, 32 m asl; ~400 km west of Akçakale cave). These data are plotted alongside isotope values of surface waters and cave waters. Predicted values of δ_w are denoted by the grey bar (see text). The global meteoric water line (GMWL) defined by Rozanski et al. (1992) and a local meteoric water line for Turkey (LMWL(T)) defined by Dirican et al. (2005) are given.

isotope composition of cave drip water ($\delta^{18}O_w$) can be calculated. Using the palaeotemperature equations of Kim and O'Neil (1997) and Anderson and Arthur (1983) for calcite deposited in a cave air temperature of +12.7 °C, with $\delta^{18}O_c$ of −10.5‰, and assuming precipitation to be in equilibrium with drip waters, predicted $\delta^{18}O_w$ using both equations are high compared to measured values of $\delta^{18}O_w$. Kim and O'Neil (1997) give values of −10.8 and Anderson and Arthur (1983) give values of −11.4‰. These data suggest either calcite precipitation that is not in isotopic equilibrium with its drip water and/or a lagged component of summer/early autumn rainfall that had

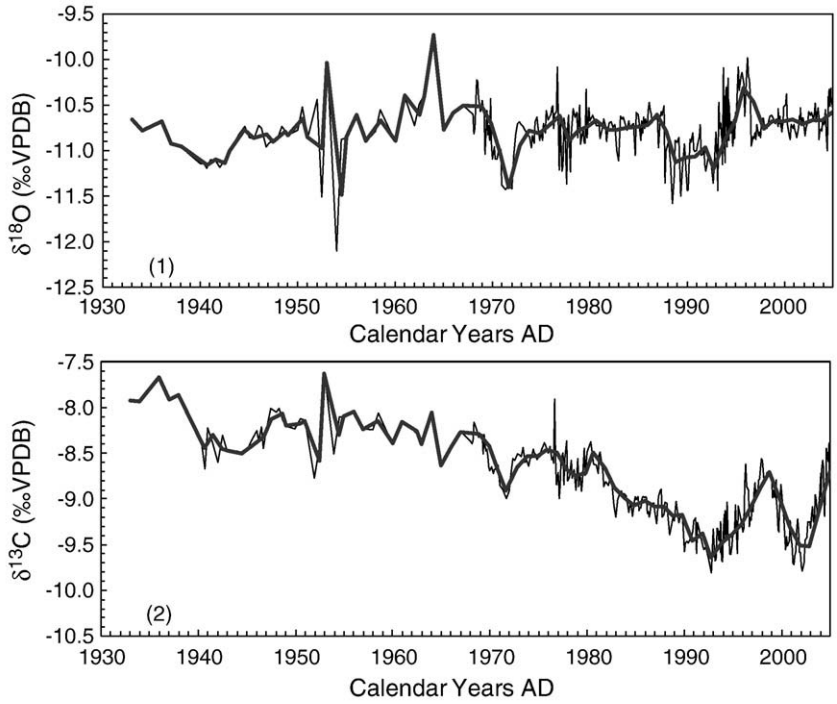

Fig. 4. Top: Stable isotope profiles of 2p. 1: $\delta^{18}O$; 2: $\delta^{13}C$. Grey line: sub-annual stable isotope profile; Black line: annually averaged stable isotope profile. An analytical error of ± 0.1‰ is assumed on all measurements. Meteorological data are available from Gümüşhane meteorological station after AD 1961.

not yet contributed to the drip water composition at the time of sampling. Nonetheless, the range of predicted $\delta^{18}O_w$ is inline with $\delta^{18}O$ of precipitation during spring to winter months at Senyurt and Dalbahce stations and snow samples from Senyurt (not shown), confirming that recharge is dominated by autumn, winter and spring precipitation, with a component of spring snowmelt.

4.3. $\delta^{18}O$ data between 1948 and 2004 AD

The sub-annual and annually averaged stable isotope data that will be used in the climate correlations are presented in Fig. 4. 2p $\delta^{18}O$ ranges by 2.4‰ from −12.1 to −9.7‰, with a mean of −10.7‰. $\delta^{13}C$ data are also presented for reference in the following section discussing isotope equilibrium.

4.4. Isotope behaviour

The Hendy test is a way of establishing whether or not a speleothem grew in isotopic equilibrium with its drip water. Isotopic equilibrium is established if there is no significant correlation between $\delta^{18}O$ and $\delta^{13}C$ along a single growth layer and an absence of progressive enrichment of ^{18}O and ^{13}C along a single lamina away from the central growth axis (Hendy, 1971). Two growth layers were sampled (in pre-instrumental calcite) for $\delta^{18}O$ and $\delta^{13}C$ and are labelled A and B in Fig. 1. The $\delta^{18}O$ and $\delta^{13}C$ data for 2p are positively correlated along both growth layers with a rank correlation coefficient of 0.94 ($p = 0.02$) in lamina A, and 0.79 ($p = 0.05$) in lamina B. Possible enrichment towards the flanks of the stalagmite is shown in lamina A only. A significant positive correlation is observed between $\delta^{18}O$ and $\delta^{13}C$ along the central growth axis in 2p ($r = +0.27$; $n = 324$; significant at 99% level in sub-annual data). Product correlations between $\delta^{18}O$ and $\delta^{13}C$ throughout a single years worth of calcite deposition (not shown) demonstrate a positive co-variation in the two isotopes over the space of a year.

Autocorrelation (i.e. the correlation of a series with its self at various lags) of the isotope data tests for a lag or memory in the system, and as such can indicate storage times in the karst aquifer and may identify the presence of low-frequency trends in the data. 2p

Table 2
Product correlation coefficients for groups of months using 100% average of the previous "x" years of precipitation data. Those significant at the 5% level are shown in bold type. Correlation coefficients of individual months correlated to $\delta^{18}O$ at t_0 and $t_{0\ to\ -5}$ are displayed, though none of these are significant (at 5% level).

Smoothing	Annual P	DJF	MAM	JJA	SON	ONDJ	ONDJF	ONDJFMA
t_0 (Jan:0.17; Feb: −0.16; Mar: −0.01; Apr: −0.05; May: 0.01; Jun: −0.05; Jul: 0.09; Aug: −0.20; Sep: 0.09; Oct: −0.22; Nov: −0.21; Dec: −0.13)	−0.20	−0.04	−0.03	−0.03	−0.23	−0.19	−0.22	−0.07
$t_{0\ to\ -1}$	−0.17	0.07	0.04	0.06	−0.36	−0.23	−0.24	−0.20
$t_{0\ to\ -4}$	−0.59	−0.38	0.04	−0.18	−0.47	−0.62	−0.60	−0.63
$t_{0\ to\ -5}$ (Jan:0.24; Feb: −0.31; Mar: 0.05; Apr: 0.21; May: −0.07; Jun: −0.15; Jul: −0.07; Aug: −0.22; Sep: 0.08; Oct: −0.37; Nov: −0.46; Dec: −0.38)	−0.61	−0.46	0.10	−0.23	−0.48	**−0.71**	**−0.67**	**−0.69**
$t_{0\ to\ -9}$	−0.35	−0.39	−0.09	−0.15	−0.02	−0.33	−0.33	−0.24

$\delta^{18}O$ is insignificantly (positively) auto-correlated (at 95% level) with a lag of up to 3 yr. This is suggestive of a short residence time of water in the karst aquifer before entering the cave as drip water. It also confirms the absence of a long term low-frequency trend in the $\delta^{18}O$ data, which if present and thought to be unrelated to a climatic parameter, would have to be removed by de-trending.

4.5. Stable isotopes vs. climate parameters

Sub-annual stable isotope data were averaged over a single year to obtain a mean annual value (VPD‰) (as shown in Fig. 4). These data are referred to as the "raw" (i.e. no supra annual smoothing applied) stable isotope proxy data. The raw proxy data was correlated (using simple product correlations) against available climate parameters, namely: precipitation (annual, seasonal and monthly totals) and temperature (annual, seasonal and monthly means). It is noted here that no significant or reliable correlations were observed between temperature (monthly, seasonal or annual) vs. $\delta^{18}O$ or $\delta^{13}C$ and between precipitation (monthly, seasonal or annual) vs. $\delta^{13}C$ in stalagmite 2p. As such these are not presented in the following sections.

Initially, product correlation coefficients were obtained between the raw stalagmite proxy data vs. the "raw" climate parameters, such that stalagmite proxy of year x was correlated against the corresponding climate parameter for that same year x. The resulting correlation coefficients ($\delta^{18}O$ vs. precipitation totals) are presented in the top row of Table 2 (correlations of individual months, annual total and seasonal totals at t_0). This assumes that the proxy value is controlled entirely by "event" water, i.e. water falling within that same year of speleothem formation. In reality, it is likely that the feeding drip waters comprise a component of this short term "event" water (i.e. a residence time of ~1 yr) and some component of stored water with a longer residence time in the karst aquifer (>1 yr). To account for this residence time of stored water, the instrumental climate data were subjected to various levels of smoothing (up to 10 yr) by taking an average of the current (t_x) and the previous x years ($t_{x\ to\ -z}$).

$$W_{tx} = (\Sigma I_{x\ to\ z}) / n \quad (1)$$

Where:

W = smoothed climate parameter (contributing to drip water at time t_x)
I = raw climate parameter
n = number of years (i.e. degree of smoothing)
x = current year; $x = -1$ to -9

For example a 10 yr smoothing of any observed climate parameter is denoted as $I_{0\ to\ -9}$ and $n = 10$. This method is from here on referred to as a "100% average" model, as it takes a simple average of the instrumental climate parameter of a group of years and correlates this to the raw proxy data. It is important to note that for the correlations between all of the proxies and climate data, $n = 43$ (AD 2004 to 1961), but once the data are smoothed, the degrees of freedom will decrease; effectively reducing the number of independent data points with increased smoothing:

$$df = \frac{n-1}{Sm} \quad (2)$$

Where:

df = degrees of freedom
n = number of data points
Sm = amount of smoothing (years)

As such, correlations will have to be large in order to be significant and a causal link between the proxy and climate parameter to be drawn. For example, with a decadal smoothing ($Sm = 10$), only correlations >0.81 are significant at the 5% significance level. Thus, smoothing beyond 10 yr is not considered here. Reduced degrees of freedom associated with smoothed data series has significance beyond speleothem calibrations and equally applies to other proxy archives. Correlations obtained using 100% average models (Table 2) show 2p $\delta^{18}O$ to be most strongly correlated ($r = -0.71$) with total late autumn–winter precipitation during the months ONDJ when smoothed by 6 yr i.e. "100% average $t_{0\ to\ -5}$".

This "100% average" model implies that the rainfall of each year contributed equally to the drip water from which the stalagmite forms. A simple mixing model was implemented by Baker et al. (2007) in order to reflect the more likely situation of relative proportions of event ($t = x$) to stored water ($t = x-1$ to z) in the emerging drip waters.

$$W_x = MI_x + (1-M)\Sigma I_{x-1\ to\ z} \quad (3)$$

Where:

x = current year; z = maximum smoothing
W = smoothed climate parameter at time $t = x$.
I = raw climate parameter at time $t = x$.
M = proportion of event water i.e. at time $t = x$.
$1-M$ = remaining stored water component i.e. at time $t = x-1$ to z

This simple "weighted" mixing model is implemented here, to further investigate the strongest correlation coefficients obtained using the "100% average" model. In the repeated correlations (for months ONDJ as these returned the highest correlation coefficient using the "100% average" model), the contribution of short term water storage (M) was varied between 30 and 5%, and longer term water storage ($1-M$) subsequently varied between 70 and 95%. The results of these repeated correlations are presented in Table 3. A marginal improvement ($r = -0.72$) was produced by a mixing model of 10% event water and 90% stored water up to 6 yr (10% t_0; 90% $t_{-1\ to\ -5}$).

The forcing mechanisms for these observed correlations between proxy data and climate parameters obtained using these two models of smoothed late autumn–winter precipitation are considered prior to applying the strongest correlations in the form of a calibration of the proxy data over the instrumental period.

Table 3
Product correlation coefficients for $\delta^{18}O$ vs. total annual and total late autumn–winter precipitation amounts based on mixing models that allow for a combination of short term (event) water and longer term (stored) water supply to the drip waters feeding stalagmite 2p. Those significant at the 5% level are shown in bold type.

Smoothing	Total annual P	Total autumn–winter P (ONDJ)
30% t_0 70% $t_{-1\ to\ -5}$	−0.54	−0.62
20% t_0 80% $t_{-1\ to\ -5}$	−0.60	**−0.70**
10% t_0 90% $t_{-1\ to\ -5}$	−0.61	**−0.72**
30% $t_{0\ to\ -1}$ 70% $t_{-2\ to\ -5}$	−0.61	−0.65
10% $t_{0\ to\ -1}$ 90% $t_{-2\ to\ -5}$	−0.59	**−0.69**
5% t_0 95% $t_{-1\ to\ -5}$	−0.60	−0.65

5. Discussion

In this region, an increase in late autumn–spring precipitation would contribute a greater amount of isotopically light storage water. Possible processes that would generate the observed correlations between total amount of effective precipitation with 2p $\delta^{18}O$ are (1) a rainfall amount effect in precipitation at this site. This cannot be demonstrated at present however, due to scarcity of precipitation

isotope data and its discontinuous nature. (2) A balance between winter and summer precipitation, when excessive summer precipitation permits infiltration into the karst aquifer. However a ratio of late autumn–winter vs. summer precipitation gives a weaker correlation of −0.20 (ONDJ:JJA vs. 2p δ^{18}O) or −0.43 (ONDJF:JJA vs. 2p δ^{18}O), neither or which are significant at 95% level, and can be ruled out. (3) Decreased disequilibrium fractionation when there is higher effective precipitation. This is plausible due to some evidence of disequilibrium (see below), though the precise driving mechanism at this stage is unknown. These processes are explored in the next sections. The correlations observed here between late autumn to spring (ONDJF and ONDJFMA) and late autumn–winter precipitation

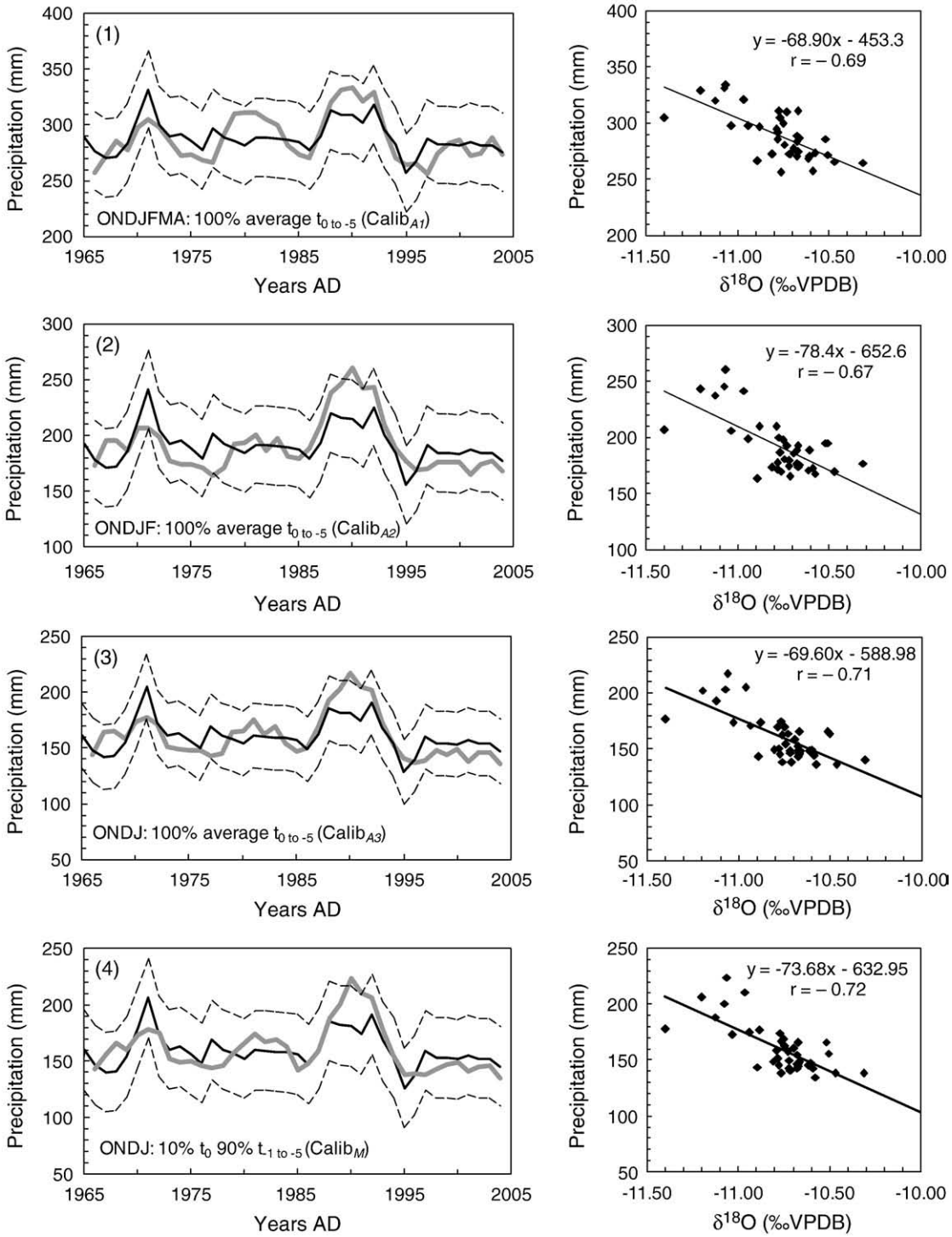

Fig. 5. Calibration of δ^{18}O with precipitation amount based on the strongest relationships observed (by product correlations): (1) late autumn to spring (ONDJFMA); (2) late autumn to early spring (ONDJF); (3) and (4) late autumn–winter (ONDJ). Two methods of smoothing the instrumental precipitation data to account for storage in the karst aquifer are presented in 1 to 3) δ^{18}O vs. precipitation amount using a simple average (calib$_{A1-3}$: 100% average $t_{0\ to\ -5}$) and in (4) δ^{18}O vs. precipitation amount smoothed over the previous 6 yr using a mixing model (calib$_M$: 10% $t_{0\ to\ -1}$; 90% $t_{-2\ to\ -5}$). Calibrated precipitation from 2p δ^{18}O is presented (black solid lines) alongside (smoothed) observed instrumental precipitation (grey solid lines). Dashed lines indicate the error limits expected with these reconstructions (±35 mm).

(ONDJ) vs. 2p $\delta^{18}O$ suggest that up to 50% of the variability in 2p $\delta^{18}O$ can be accounted for using a "100% average" model smoothed by 6 yr ("100% average $t_{0\ to\ -5}$"). Using a mixing model for late autumn–winter months only ("ONDJ 10%t_0; 90% $t_{-1\ to\ -5}$"), 51% of the variability of 2p $\delta^{18}O$ may be accounted for. The residual 49 to 50% can be speculatively explained by other factors.

5.1. Correlations with $\delta^{18}O$

In summer (later spring and early autumn) circulation is generally from the north or north-west with the Asian low drawing down winds over the Black Sea and onto the Black Sea coast (Kutiel et al., 1998; Kutiel and Maheras, 1998; Kadıoğlu, 2000), with large amounts of isotopically heavier rain on the windward side of the Kaçkar mountains (Dirican et al., 2005). Akçakale cave is located in the rain shadow of such air masses. Further, from June to September there is a soil moisture deficit and reduced precipitation totals, so rain falling in these months is likely to have a minimal contribution to storage water. The co-variation between the two isotopes during the course of a single year was observed by Jex (2008) for some laminae, suggesting seasonal variability in isotope content recorded in 2p, however the mean annual isotope content presented here is dominated by the late autumn–spring and in particular, the ONDJ precipitation signal.

5.2. Stable isotope behaviour and residence time of drip waters

The possibility of kinetic fractionation during the formation of speleothem 2p is suggested by the co-variation of the two isotopes through time in 2p (Hendy, 1971). Kinetic fractionation of drip waters results in stable isotope compositions of calcite out of equilibrium with their feeding drip waters and may occur due to rapid degassing when drip water is super saturated or due to evaporation of drip water on the cap of the stalagmite when cave humidity is low (Mickler et al., 2004). Relative humidity in Akçakale was measured between 95 and 98%, suggesting limited or no fractionation due to evaporation of drip water. Conditions suitable for rapid degassing with calcite forming out of equilibrium with its drip water are however suggested by the fast drip rates observed for 2p, and high (synthetic) SI_c of its drip waters (Section 3). This could be driven seasonally by seasonal variation in drip water pCO_2.

According to the correlation data, 2p drip waters are supplied by an aquifer recharged by waters from the current year and the previous 5 yr (any older than this and correlations decrease). This short residence time is confirmed by the short lag in the auto correlation of 2p $\delta^{18}O$.

5.3. Calibrated late autumn–winter precipitation amount over the instrumental period

2p $\delta^{18}O$ has been calibrated with ONDJFMA ($calib_{A1}$), ONDJF ($calib_{A2}$) and ONDJ ($calib_{A3}$) precipitation for the fitting period 1961 to 2004 AD smoothed by an average of 6 yr ($calib_{A1-3}$: 100% average $t_{0\ to\ -5}$). The strongest correlation coefficient was observed between 2p $\delta^{18}O$ and ONDJ precipitation. This was investigated further, using a mixing model to account for differing residence times of water in the karst aquifer before entering the cave as drip water ($calib_M$: 10% t_0; 90% $t_{-1\ to\ -5}$). The scatter plots of these relationships are shown in Fig. 5, and contain few outliers that would significantly alter the correlations. The calibrations are also presented in Fig. 5. As such they both present a

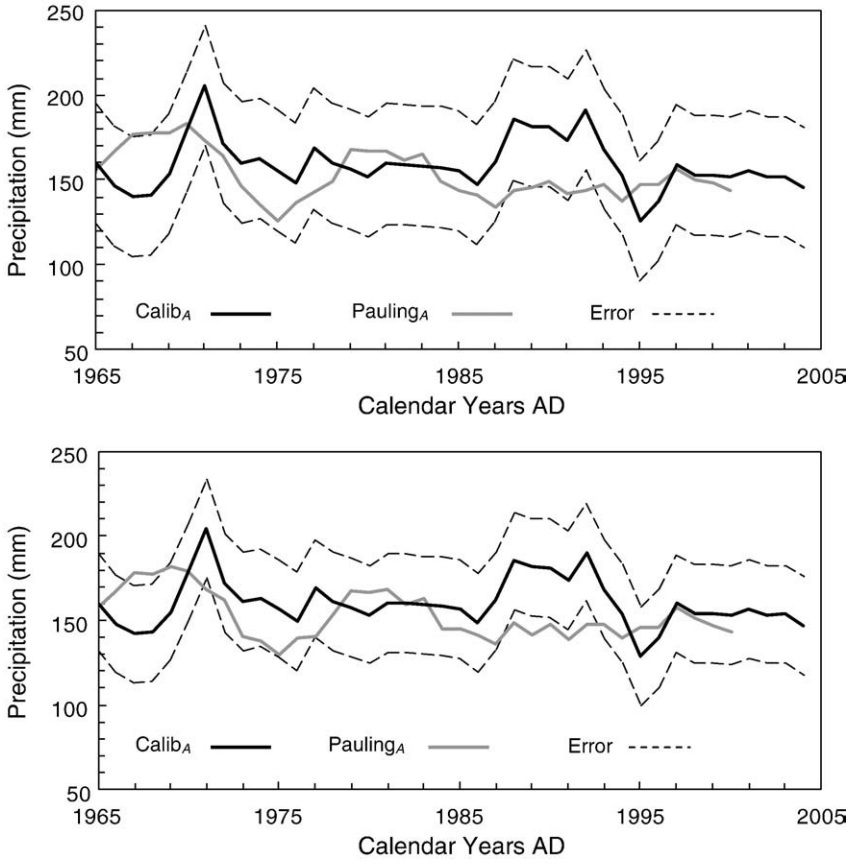

Fig. 6. Comparison of ONDJ $calib_M$ (top) with total winter precipitation predicted by Pauling et al. (2006) (smoothed using the mixing model $_M$) and ONDJ $calib_{A3}$ (bottom) with the Pauling et al. regional winter precipitation reconstruction smoothed using mixing model $_A$. (Pauling et al. (2006) data were obtained from the Climate Explorer Website). Dotted lines represent maximum and minimum estimated errors (2 standard errors) associated with $calib_M$ and $_{A3}$.

smoothed record (6 yr) with associated errors of ±35 mm (2 standard errors on the regression).

Whilst capturing the general trends of precipitation over this period, all calibrations under predict the peak in rainfall of the early 1990s (1990 to 1992) and fail to capture the small decrease in precipitation in the late 1970s. The calibrations capture the general shape and timing of the two largest precipitation peaks in 1971 and 1991, though over predict and under predict the magnitude of each respectively. The peak in rainfall between 1981 and 1983 is not captured particularly well in either calibration. Noticeably, the speleothem calibrated data for ONDJFMA do not record the increase in spring precipitation in the mid 1970s.

There appears to be no major advantage of using the more complicated calib$_M$ (which only returned a marginal improvement on the correlation coefficient between ONDJ precipitation and δ^{18}O) over the computationally simpler calib$_A$. Further, whilst a mixing model allowing for a weighted contribution of event and stored water to the feeding drips may initially seem preferable to a simple average model, it is not without issues. Specifically, it is unlikely that the proportion of event: stored water used in the model has remained constant over the fitting period of the calibration (and even less so over any time period prior to this calibration, which becomes relevant if a reconstruction based on this relationship is sought).

Calib$_M$ and $_{A3}$ are illustrated in Fig. 6, plotted against the Pauling et al. (2006) historical winter precipitation reconstruction for longitude: 35 to 40°N and latitude 30 to 40°E (data available at: http://climexp.knmi.nl; Accessed: March 2008). This provides an initial (qualitative) verification of this record and its regional applicability. There is a reasonable consistency (within errors) in the direction and magnitude of the precipitation trends of the two calibrations and the Pauling et al. (2006) record, with the speleothem record lagging the historical reconstruction by 1 or 2 yr. Between AD 1986 and 1995 the observed late autumn–winter precipitation record at Gümüşhane and calibrated speleothem record show a large increase in precipitation, which is absent in the Pauling et al. (2006) record. After AD 1995 all series converge.

As highlighted by Baker and Bradley (2010-this issue), the main limiting factor currently associated with the linear regression models of calib$_M$ and $_A$, is due to the reduced degrees of freedom once storage in the karst aquifer is accounted for. Future validation of these calibration models would go some way towards reducing this.

6. Conclusions

The strongest and most consistent correlation is between 2p δ^{18}O and the total amount of late autumn–winter (ONDJ) precipitation with a 6 yr smooth.

A calibration based on a mixing model to allow for varying residence time of stored waters prior to entering the cave as drip water (calib$_M$), offers no advantage over the computationally simpler "100% average" model (calib$_A$). Extended calibrations are as yet unverified beyond the fitting period (1961 to 2005 AD) but demonstrate a reasonable coherence with the regional reconstruction of Pauling et al. (2006) for the same region.

Possible causes for the strong correlation between ONDJ (ONDJF and ONDJFMA) precipitation and δ^{18}O of 2p have been put forward. Recharge of the karst aquifer is dominated by isotopically light late autumn–winter (and spring) precipitation. It is likely recharged slowly during autumn and winter, then more rapidly in spring due to melting of snow and ice that accumulate during the winter. There is evidence of spring rains contributing to drip waters, but weaker correlation coefficients suggest that late autumn–winter precipitation dominates the isotope signal recorded in stalagmite 2p. Possible causes for these correlations are suggested to be due to a rainfall amount effect in precipitation at this site (though precipitation isotope data is not of sufficient quantity or continuous enough to either confirm or disprove this) and/or decreased disequilibrium fractionation when there is higher effective precipitation (though the exact mechanism that would drive this is presently not known).

Kinetic fractionation is suggested in the drip waters feeding 2p, due to a sub-annual co-variation in δ^{13}C and δ^{18}O isotopes, positive Hendy tests, and further evidence from modern drip waters, including high SI$_c$ indices and a potential seasonal lag inferred in drip water δ^{18}O by palaeotemperature equations. Nonetheless, sensible calibrations of speleothem δ^{18}O with precipitation amount have been obtained.

The speleothem reconstructions presented here require validation beyond the calibration period (i.e. by cross-validation techniques over the fitting period or by obtaining an extended record of Gümüşhane precipitation against which to verify the calibration prior to 1961 AD). Nevertheless it is an encouraging start in understanding trends in moisture availability in NE Turkey over the instrumental period and provides a basis upon which future research will allow isotope records of the last 500 yr to be interpreted in terms of moisture availability.

Acknowledgments

This research was funded by the School of Geography, Earth and Environmental sciences at The University of Birmingham; NERC Isotope Geosciences Laboratory at the British Geological Survey, Keyworth, UK (allocation no. IP/877/2005); with financial assistance from the British Institute of Archaeology at Ankara (study grant) and field work funded as part of grants awarded to the ENVΔNET project (Environmental Change North East Turkey). The authors acknowledge the Turkish Environment and Forestry Ministry (Çevre ve Orman Bakanlığı) and the tourism department and officials of Gümüşhane local government for permission to work at Akçakale cave.

References

Anderson, T.F., Arthur, M.A., 1983. Stable isotopes of oxygen and carbon and their application to sedimentologic and paleoenvironmental problems. In: Arthur, M.A. (Ed.), Stable Isotopes in Sedimentary Geology, pp. 1–151.

Baker, A., Bradley, C., 2010. Modern stalagmite δ^{18}O: instrumental calibration and forward modelling. Global Planetary Change 'MedClivar Special Issue' 71, 201–206.

Baker, A., Genty, D., Dreybrodt, W., Barnes, W.L., Mockler, N.J., Grapes, J., 1998. Testing theoretically predicted stalagmite growth rate with recently annually laminated samples: implications for past stalagmite deposition. Geochimica et Cosmochimia Acta 62 (3), 393–404.

Baker, A., Asrat, A., Fairchild, I.J., Leng, M.J., Wynn, P.M., Bryant, C., Genty, D., Umer, M., 2007. Analysis of the climate signal contained within δ^{18}O and growth rate parameters in two Ethiopian stalagmites. Geochemica et Cosmochimica Acta 71, 2975–2988.

Baker, A., Smith, C.L., Jex, C., Fairchild, I.J., Genty, G., Fuller, L., 2008. Annually laminated speleothems. International Journal of Speleology 37 (3), 193–206.

Banner, J.L., Guilfoyle, A., James, E.W., Stern, L.A., Musgrove, M., 2007. Seasonal variations in modern speleothem calcite growth in central Texas, U.S.A. Journal of Sedimentary Research 77 (8), 615–622.

Dirican, A., Ünal, S., Acar, Y., Demircan, M., Dirican, A., Ünal, S., Acar, Y., Demircan, M., 2005. The temporal and seasonal variation of H-2 and O-18 in atmospheric water vapour and precipitation from Ankara, Turkey in relation to air mass trajectories at the Mediterranean Basin. IAEA, 2005. Isotopic Composition of Precipitation in the Mediterranean Basin in Relation to Air Circulation Patterns and Climate.

Dreybrodt, W., 1988. Processes in Karst Systems, Physics, Chemistry, and Geology. Springer-Verlag.

Fairchild, I.J., Smith, C.L., Baker, A., Fuller, L., Spötl, C., Mattey, D., McDermott, F., E.I.M.F., 2006. Modification and preservation of environmental signals in speleothems. Earth Science Reviews 75, 105–153.

Ford, D.C., Williams, P., 2007. Karst Hydrogeology & Geomorphology. John Wiley & Sons.

Frisia, S., Badertscher, S., Borsato, S., Susini, J., Göktűrk, OM., Cheng, H., Edwards, RL., Kramers, J., Tüysüz, O., Fleitmann, D., 2008. The use of stalagmite geochemistry to detect past volcanic eruptions and their environmental impacts. PAGES News 16 (3), 25-25.

Fuller, L., Baker, A., Fairchild, I.J., Spötl, C., Marca-Bell, A., Rowe, P., Dennis, P.F., 2008. Isotope hydrology of dripwaters in a Scottish cave and implications for stalagmite palaeoclimate research. Hydrology and Earth System Sciences 12, 1065–1074.

Genty, D., Deflandre, G., 1998. Drip flow variations under a stalactite of the Père Nöel cave (Belgium). Evidence of seasonal variations and air pressure constraints. Journal of Hydrology 2111, 208–232.

Genty, D., Baker, A., Barnes, W.L., 1997. Comparison entre les lamines luminescentes et les lamines visibles annualles de stalagmites. Cómptes Rendus de l'Academie des Sciences 325, 193–200.
Hendy, C.H., 1971. The isotopic geochemistry of speleothems: the calculation of the effects of different modes of formation on the isotopic composition of speleothems and their applicability as palaeoclimatic indicators. Geochimica et Cosmochimica Acta 35 (8), 801–824.
IAEA/WMO, 2006. Global network of isotopes in precipitation. The GNIP Database. Accessible at: http://isohis.iaea.org.
IPCC. (2007) Climate change 2007: synthesis report. Contribution of Working Groups I, II and III to the Fourth Assessment Report of the Intergovernmental Panel on Climate Change [Core Writing Team, Pachauri, R.K and Reisinger, A. (eds.)]. IPCC.
Jex, C, N. (2008) Speleothem palaeoclimate reconstructions from north east Turkey, PhD, The University of Birmingham, UK.
Kadıoğlu, M., 2000. Regional variability of seasonal precipitation over Turkey. International Journal of Climatology 20 (14), 1743–1760.
Kim, S., O'Neil, J.R., 1997. Equilibrium and nonequilibrium oxygen isotope effects in synthetic carbonates. Geochimica et Cosmochimica Acta 61 (16), 3461–3475.
Krüger, Y., Fleitmann, D., Frenz1, M., 2008. Paleotemperatures from fluid inclusion liquid–vapor homogenization in speleothems. PAGES News 16 (3), 13–14.
Kutiel, H., Maheras, P., 1998. Variations in the temperature regime across the Mediterranean during the last century and their relationship with circulation indices. Theoretical and Applied Climatology 61 (1), 39–53.
Kutiel, H., Maheras, P., Guika, S., 1998. Singularity of atmospheric pressure in the eastern Mediterranean and its relevance to interannual variations of dry and wet spells. International Journal of Climatology 18, 317–327.
Kutiel, H., Hirsch-Eshkol, T.R., Türkes, M., 2001. Sea level pressure patterns associated with dry or wet monthly rainfall conditions. Theoretical Applied Climatology 69, 39–67.
Lachniet, M., 2009. Climatic and environmental controls on speleothem oxygen-isotope values. Quaternary Science Reviews 28 (5–6), 412–432.
McDermott, F., 2004. Paleo-climate reconstruction from stable isotope variations in speleothems: a review. Quaternary Science Reviews 23, 901–918.
McDermott, F., Schwarz, H., Rowe, P.J., 2006. Isotopes in speleothems. In: Leng, M.J. (Ed.), Isotopes in Palaeoenvironmental Research. Springer, pp. 227–273.
Mickler, P.J., Banner, J.L., Stern, L., Asmerom, Y, Edwards, R., Ito, E., 2004. Stable isotope variations in modern tropical speleothems: evaluating equilibrium vs. kinetic isotope effects. Geochimica et Cosmochimica Acta 68 (21), 4381–4393.
Nazik, L., 1994. Natural caves of Gumushane and Bayburt region. Second Symposium of Speleology, MTA.
Pauling, A., Luterbacher, J., Casty, C., Wanner, H., 2006. Five hundred years of gridded high-resolution precipitation reconstructions over Europe and the connection to large-scale circulation. Climate Dynamics 26, 387–405.
Robinson, A.G., Banks, C.J., Rutherford, M.M., Hirst, J.P.P., 1995. Stratigraphic and structural development of the Eastern Pontides, Turkey. Journal of the Geological Society 152 (5), 861–872.
Rozanski, K., Araguas-Araguas, L., Gonfiantini, R., 1992. Relation between long-term trends of oxygen-18 isotope composition of precipitation and climate. Science 258 (5084), 981–985.
Smith, C. (2006) The statistical analysis of speleothem palaeoclimate records. PhD, The University of Birmingham, UK.
Statistical Yearbook of Turkey (Turkiye istatistik yilligi) (2002). State Institute of Statistics Prime Ministry Republic of Turkey, Ankara.
Tan, M., Baker, A., Genty, D., Smith, C., Esper, J., Cai, B., 2006. Applications of stalagmite laminae to paleoclimate reconstructions: comparisons with dendrochronology/climatology. Quaternary Science Reviews 25, 2103–2117.
Thornthwaite, C.W., 1948. An approach toward a rational classification of climate. Geographical Review 38 (1), 55–94.
Thornthwaite, C., 1957. Instructions and tables for computing potential evapotranspiration and the water balance. Publication in Climatology: Lab. Climatol. Dresel Inst. Technol., vol. 10(3), pp. 185–311.
Treble, P.C., Chappell, J., Gagan, M.K., McKeegan, K.D., Harrison, T.M., 2005. In situ measurement of seasonal $\delta^{18}O$ variations and analysis of isotopic trends in a modern speleothem from southwest Australia. Earth and Planetary Science Letters 233 (1–2), 17–32.
Unal, Y., Kindap, T., Karaca, M., 2003. Redefining the climate zones of Turkey using cluster analysis. International Journal of Climatology 23, 1045–1055.